

# Role of initial density distribution in simulations of bone remodeling around dental implants

EMIL NUȚU<sup>1,2\*</sup>

<sup>1</sup> University Politehnica of Bucharest, Faculty of Engineering and Management of Technological Systems,  
Strength of Materials Department, Bucharest, Romania.

<sup>2</sup> Romanian Research and Development Institute for Gas Turbines COMOTI,  
Research and Development for Satellites and Space Equipment Department, Bucharest, Romania.

*Purpose:* In this paper, the effect of initial density distribution upon the predicted density via numerical simulations of bone remodeling was evaluated. The main purpose was to correlate the numerical results with clinical data according to which the initial bone quantity is an essential factor for long term survival of dental implants. *Methods:* Two-strain energy density-based bone remodeling theories were employed, one which accounts for overload resorption and the second one, which does not. The remodeling parameters were derived from the mechanostat theory. Bone remodeling around an osseointegrated dental implant was simulated based on finite element method using a generic mandible plane model. A variable time step was introduced to increase the speed of the remodeling simulations by keeping the truncation errors small. The simulations were performed for several initial density distributions correlated with values from clinical classifications of bone quality. For each density value, the occlusal load was defined in two ways so that to consider normal and overload mastication forces, respectively. *Results:* The results showed that the initial density distribution influences the predictions of bone remodeling simulations. For the analyzed model, the remodeling algorithm predicted overload resorption only in the case of low initial density, which can be associated with low bone quality, which, from clinical perspective, may probably lead to implant loss. *Conclusions:* The paper demonstrated that when simulating bone remodeling around dental implants using finite element method, it is important to account for initial density distribution in correlation with the bone quantity.

*Key words:* strain energy density, bone quantity, initial conditions, bone remodeling simulation

## 1. Introduction

Dental implants are used to replace the teeth roots of edentulous patients in order to provide support for dental prosthesis. The placement of such devices within bone is an invasive procedure which determines the processes of bone healing and remodeling to occur [12]. Bone healing lasts up to 6 months [20] and involves new bone formation around and on the implant, determining the so-called implant osseointegration. Bone remodeling (BR) is a long-lasting process which begins during the healing period [12] and takes place for the rest of life. It involves an increase of bone mass in the areas with higher stresses via a sub-

process called bone formation (BF) and a decrease where the stresses are low throughout the subprocess known as bone disuse resorption (DR) or underload resorption [4]. Thus, bone cells react to mechanical stimuli by maintaining an optimum bone mass which is needed to ensure mechanical support. If locally more bone is needed due to high loads, BF occurs and if too much bone locally exist to sustain small loads, the bone is resorbed away by DR mechanism. However, bone deposition does not occur at unlimited high loads. Over a certain limit of stresses, bone overload resorption (OR) occurs [8].

Prior to implant placement, clinicians investigate the structure of bone in the surgical area in order to ensure mechanical support for the dental prosthesis.

---

\* Corresponding author Emil Nuțu, University Politehnica of Bucharest, Sector 6, Spaiul Independenței, No 313, RO-060042, Bucharest, Romania. E-mail address: Phone: +40721 271 299, e-mail: emil.nutu@upb.ro

Received: August 18th, 2018

Accepted for publication: October 18th, 2018

The density of bone in the investigated region is termed bone quantity (BQ) [13]. It is known that the BQ is an important factor for implant success [13], [15], i.e., long term implant survival. Higher chances of implant failure due to overloading by high mastication forces are associated with lower bone densities [15].

Numerical bone remodeling theories were successfully applied demonstrating the ability of algorithms to predict density distributions around dental implants resembling the actual bone architecture [2]. The simulation of BR starts from an initial density distribution which is usually considered constant over the simulation domain [2], [11]. By correlating the Young's modulus with the density via empirical expressions [6], an initial constant rigidity of the trabecular architecture is defined. However, different initial Young's modulus, which mimic the initial BQ, determines a different stress distribution as the local rigidity influences load transfer within statically indeterminate systems. In the case of mathematical BR models which do not account for OR, the higher the load applied, the higher the predicted density. Such results are not consistent with the clinical data according to which the overloading is a potential cause of implant loss due to OR [22]. However, if the OR is accounted for, as some mathematical models employ it [8], [21], it is likely to obtain different density distributions, depending on the initial Young's modulus selection.

Based on the above observations, the aim of this work was to simulate BR around dental implants using different initial conditions (initial Young's modulus) correlated with clinical bone quantity. It is of interest to check whether the initial Young's modulus influences the density predictions in the sense that clinical outcomes report, i.e., higher implant loss rate in the low quantity bone. There are employed two commonly used mathematical models of BR, based on Huiskes et al. [7] formulation in which the strain energy density (SED) is the mechanical driving stimulus. The first model accounts only for the DR and BF, while the other is also capable of simulating OR. The simulations are performed on a plane model that represents an occlusal section of a generically shaped mandible. Also a generic implant is considered.

## 2. Methods

### *Bone remodeling theories*

Following Huiskes et al. [7], the BR equation without OR capability is given in:

$$\frac{d\rho}{dt} = \begin{cases} B[S - S_o(1-w)], & S < S_o(1-w) \\ 0, & S_o(1-w) \leq S \leq S_o(1+w), \\ B[S - S_o(1+w)], & S > S_o(1+w) \end{cases} \quad (1)$$

where  $\rho$  is the apparent density which includes tissue and pores,  $B$  is a constant indicating the rate of remodeling,  $S$  a measure of the mechanical stimulus that bone cells are supposed to detect and  $S_o$  a reference homeostatic value of the mechanical stimulus. Equation (1) also incorporates the so-called *lazy zone*, which is an extension of the equilibrium stimulus to an interval of no remodeling values, with the width  $2w$ .

In order to account for the OR effect, Lin et al. [8] added a quadric term to the Eq. (1), but with no lazy zone ( $w = 0$ ), as in the form:

$$\frac{d\rho}{dt} = B(S - S_o) - D(S - S_o)^2, \quad (2)$$

where  $D$  is a parameter adjustable as a function of  $B$  and  $S_o$ , so that the quadric term influence to be significant at physiologically high loads, i.e., stresses over certain values which bone is supposed to normally sustain. Therefore, Eq. (2) predicts resorption over such loading values, while Eq. (1) predicts unlimited density growth.

In this paper, a simple extension of the Eq. (2) is employed to account for overload resorption, by introducing the lazy zone, as follows:

$$\frac{d\rho}{dt} = \begin{cases} B[S - S_o(1-w)], & S < S_o(1-w) \\ 0, & S_o(1-w) \leq S \leq S_o(1+w) \\ B[S - S_o(1+w)] - D[S - S_o(1+w)]^2, & S > S_o(1+w) \end{cases} \quad (3)$$

The rate of remodeling corresponding to the two mathematical models were graphically presented in Fig. 1a and b, for a more intuitive understanding.

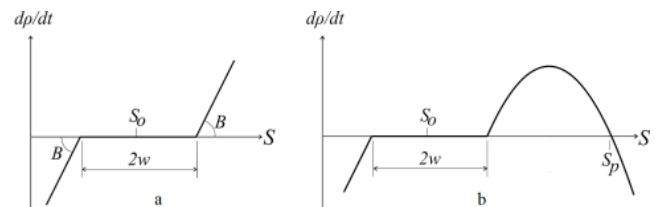


Fig. 1. Remodeling rate variation in the case of BR models:  
a – without OR and b – with OR

It is noteworthy that the OR quadric term was only introduced within the range of driving stimuli exceeding the equilibrium interval, thus in which the overload is likely to occur. A similar approach was presented by Hassan et al. [5], with the difference that

the quadric term was also included within the range of driving stimuli bellow the equilibrium interval. The third branch of Eq. (3) has only a root within its applicability range. This root has the meaning of the SED threshold at which the remodeling rate becomes negative, thus the OR occurs. Denoting it with  $S_p$ , from Eq. (3), it follows that:

$$S_p = \frac{B}{D} + S_o(1+w). \quad (4)$$

As in most studies, the mechanical stimulus was expressed as strain energy per unit of bone mass (SEM), based on:

$$S = \frac{U}{\rho}, \quad (5)$$

where  $U$  is the SED.

The Young's modulus was correlated with the apparent density following Carter et al. [1] via the expression:

$$E = 3790 \rho^3. \quad (6)$$

#### The remodeling algorithm and parameters

The two above-mentioned theories were coupled with the finite element method (FEM) using MATLAB 7 (MathWorks, Inc.) and ANSYS 18 (Ansys, Inc.). Two interconnected codes were developed: one (in MATLAB) for the evaluation of the remodeling process and the other using APDL (Ansys Parametric Design Language) for the finite element analysis (FEA).

As in most studies, the integration of bone remodeling equation was based on forward Euler scheme, being accurate enough for this kind of simulations [16]. Thus, the density update follows the rule:

$$\rho_{n+1} = \rho_n + \frac{\Delta t(i)d\rho}{dt}, \quad (7)$$

where  $\Delta t(i)$  is the time step defined in this paper as a function of the iteration index  $i$ . Other studies [2], [5], [7], [8], [11] considered a constant integration step, which, in the case of a large value, determines large truncation errors and in the case of small values, too many iterations are needed for convergence to be achieved. The basic idea was to keep an integration step small enough at the beginning of the simulation, when the density variation is high, so that the large truncation errors can be avoided. As the BR simulation progresses, the density variation diminishes substantially. A higher integration step in this case would not significantly affect the convergence be-

haviour. Following these arguments, the time step was defined as:

$$\Delta t = \frac{i}{d}, \quad (8)$$

where  $d$  is a positive integer which allow for controlling the speed of time step growing. According to Lin et al. [11], if a unity time step is chosen to represent one month, then the speed constant  $B$  should be equal to  $120 \text{ month}\cdot\text{g}/\text{cm}^5$ , so that one iteration is to equate one month of BR. Thus, if  $T$  is the total number of iterations, in the case of a one month time span, it is equal to the number of BR months. For the variable time span given by expression (8), if  $B = 120 \text{ month}\cdot\text{g}/\text{cm}^5$ , than, in order to achieve  $T$  months of BR simulation, the number,  $n$ , of necessary iterations can be determined from:

$$\frac{1}{d} \sum_{i=1}^n n = T. \quad (9)$$

Thus, it follows that

$$n = \frac{-1 + \sqrt{1 + 8dT}}{2}. \quad (10)$$

After several numerical tests, for  $B = 120 \text{ month}\cdot\text{g}/\text{cm}^5$ ,  $d$  was chosen equal to 1200. Therefore, one month of BR simulation was achieved after  $n = 49$  iterations.

The other parameters of the remodeling equation were derived from the mechostat theory of Harold Frost [4]. According to this theory, bone mass is regulated by strain magnitude. Between  $200 \mu\epsilon$  and  $1500 \mu\epsilon$ , an equilibrium strain range was defined, i.e., no bone mass change was determined. This interval of strains is equivalent with the lazy zone, thus it follows that  $w = 0.57$ . Under  $200 \mu\epsilon$ , bone exhibits DR, while over  $1500 \mu\epsilon$ , mass growth was determined by new BF. If strains exceeds  $3000 \mu\epsilon$ , it can be assumed that microdamage growth overcomes the capacity of bones to repair itself, corresponding to a pathological condition. In Frost's theory, the strain direction is not discussed. In this paper, the mechanostat thresholds were equated with von Mises strains and converted into SED values, under the linear elasticity hypothesis. Assuming a tissue density  $\rho_t = 1.54 \text{ g}/\text{cm}^3$  [10], from the mean strain value of mechanostat equilibrium interval, one can determine that the targeted SEM is  $S_0 = 0.0045 \text{ J}/\text{g}$ . The value of  $S_p$  threshold is thought to correspond to the pathological strain magnitude. Thus,  $S_p = 0.035 \text{ J}/\text{g}$ . From Eq. (4), it follows that  $D = 4296 \text{ month}\cdot\text{J}/\text{cm}^5$ . The minimum allowed value for density was taken as  $\rho_{\min} = 0.1 \text{ g}/\text{cm}^3$ .

### Initial conditions

Roy et al. [18] addressed bone quantity as initial Young's modulus distribution in finite element simulations around dental implants to select the optimal dental geometry that best suits the different bone quantities. They defined five different bone quantities based on statistical estimation from 89 patients' CT scans, considering the average as normal. In this paper, the initial quantity was introduced following Norton and Gamble [15] who defined three levels of trabecular bone density, correlated with clinical bone quantity. Based on CT data, on the Hounsfield scale, the corresponding density range was: greater than 850 HU – for quantity 1 (Q1 – high), 500..850 HU – for quantity 2 (Q2 – average) and 0..500 HU – for quantity 3 (Q3 – low). In this paper, the HU values were converted into density units [ $\text{g}/\text{cm}^3$ ], using the empirical relation [19]

$$\rho = (1.067 \text{ HU} + 131) \cdot 10^{-3}. \quad (11)$$

The initial Young's modulus was further determined from Eq. (6). The intervals for each BQ are given in Table 1.

Table 1. Correlation of bone quantity and initial conditions intervals

Clinical interpretation: BQ estimation	Imaging interpretation: Tissue radiodensity, RD [HU]	Mechanical interpretation: Apparent Young modulus, $E$ [MPa]
High (Q1)	$\text{RD} > 850$	$E > 4238$
Medium (Q2)	$500 < \text{RD} < 850$	$1114 < E < 4238$
Low (Q3)	$0 < \text{RD} < 500$	$9 < E < 1114$

For Q1 bone, the simulations were performed using initial young moduli  $E_1 = 5000$  MPa. For Q2 and Q3, the average values of Young's moduli were used over the corresponding intervals from Table 1, being considered representative for each BQ. Thus, the initial Young's moduli were  $E_2 = 2676$  MPa for Q2 and  $E_3 = 561$  MPa for Q3.

### The finite element model

A plane model of an occlusal section was considered, as presented in Fig. 2. A generic geometry is created based on the dimensions given in [2]. Two bony material regions, corresponding to cortical (the outer layer) and trabecular bone types, were defined. The remodeling process was simulated only within the trabecular region. Also, a generic implant shape was employed, with the dimensions and the threat type taken from [3] (Fig. 3).

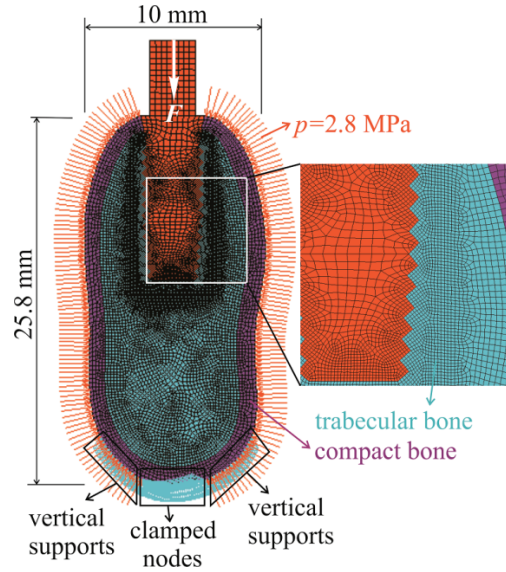


Fig. 2. Plane model of the implant – mandible assembly

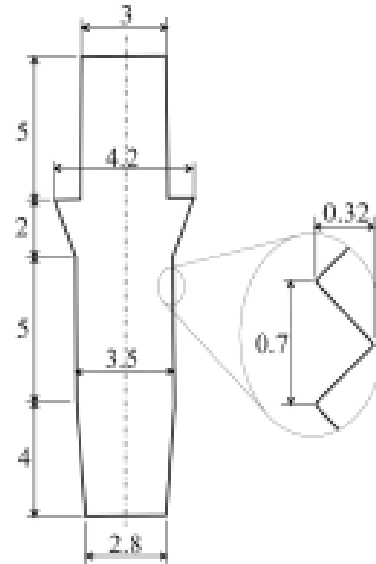


Fig. 3. Generic shape implant and its dimensions [mm]

An 8-noded plane element was used, with the plain strain option, as in [2]. In the remodeling region, the average element edge length dimension was 0.15 mm, with 0.1 mm around the implant to better capture the threat influence (Fig. 2). The implant and the surrounding bone were considered perfectly bonded, assuming that the implant was osseointegrated, i.e., the healing was achieved. Following other studies [2], [5], the outer contour of the cortical shell was loaded with a constant pressure to account for the entire mandible action upon the considered part. A value of 2.8 MPa was applied, chosen in order to the von Mises strains over the most trabecular region to be between  $200 \mu\epsilon$  and  $1500 \mu\epsilon$  (bone maintenance interval according to Frost), for all the initial densities, in

absence of the implant load. The implant was loaded with an axial force, uniformly distributed over the implant top line. In order to account for a normal mastication load and for a situation that may produce local bone overload, there are employed two force magnitudes of 100 N and 200 N, respectively. The two values were chosen from the range of 42 N and 400 N which were estimated to be the average human bite [9]. The cortical shell had a thickness of 1 mm as in paper [2] and a Young's modulus of 13.8 GPa, as deduced from relation (4) for a tissue density of  $1.54 \text{ g/cm}^3$ . The implant material was considered to be a titanium alloy, thus with Young's modulus of 110 GPa. The Poisson's ratio, for all the regions, including trabecular (remodeling space), compact and implant, was taken as 0.3.

12 cases using different BQ, initial conditions and occlusal loads were analyzed, as presented in Table 2.

Table 2. Analyzed cases

BQ	BR model	$F$ [N]	Case name
Q1	With OR	100	Q1ORF1
		200	Q1ORF2
	No OR	100	Q1NORF1
		200	Q1NORF2
Q2	With OR	100	Q2ORF1
		200	Q2ORF2
	No OR	100	Q2NORF1
		200	Q2NORF2
Q3	With OR	100	Q3ORF1
		200	Q3ORF2
	No OR	100	Q3NORF1
		200	Q3NORF2

### 3. Results

In Figures 4–6, for all the analyzed cases, the results were given in terms of density distributions, corresponding to one month and 12 months remodeling periods. One can notice that only in the case of Q3 trabecular bone and high load (Fig. 6), the algorithm predicted local OR occurring up to one-month simulation time, near the implant apex. Up to one year, the OR extended along the implant vicinity, indicating risk of implant loss. Due to the redistribution of bone stiffness via remodeling, the force transfer from implant to bone follow new formed paths which have higher stiffness, attracting thus local density growth. Therefore, the total trabecular mass

slightly increased compared to the initial value, as can be seen in Fig. 7.

For the Q1 bone, the final density distributions (one year) that correspond to the same loading conditions were similar (Fig. 4). However, there were differences regarding the total trabecular mass variation and its final value. For the 100 N occlusal load, one can notice from Fig. 7 that the mass diminished compared to the initial value. It seemed that the loading was low compared to the bone maintenance interval of SED values. This condition determined DR within the regions with SED bellow  $S_o(1 - w)$ . In the model without OR the mass dropped more rapidly than in the case with OR and the final value was smaller with 7% indicating that more bone had resorbed away. It can be deduced that, at the beginning of the simulation, the OR model generated local OR determining redistribution of loads within trabecular bone also throughout regions with low initial SED. Therefore, the SED increased in these regions generating local BD instead of DR and an overall mass decrease reduction. For the 200 N occlusal load, the smaller differences between the two models were registered. Only the mass variation with time was different, once again indicating a more rapid mass diminish in the case of model without OR, although the final values were almost the same. It can be concluded that the OR model tends to generate more uniformly distributed density by reducing high and low SED concentrations.

The Q2 trabecular bone model behaved similarly for the 100 N force load, regardless the OR term. The same final density distributions (Fig. 5) and mass variation during simulation time (Fig. 7) were registered. However, although the mass was the same for each iteration, Fig. 5 indicated faster redistribution of densities after one month for the model without OR. Admittedly it can be explained in the same way for the Q1 model. Similar observations can be applied for the 200 N cases, except for the mass variation, which, as for the Q1 bone, showed a faster and higher mass diminishing for the model without OR.

Similar behavior was registered between Q3 models, except for the one with OR and 200 N force, discussed above. It is interesting to notice that high density bone struts tended to form (Fig. 6) instead of a more homogenous distribution, as obtained for Q1 and Q2 bone types. Due to local high density of these struts, the force transfer from implant to bone was mainly achieved through those areas which have the capacity of transferring both force values. This caused no need for supplementary increase of density in the case of higher force, as one can deduce from Figs. 6 and 7.

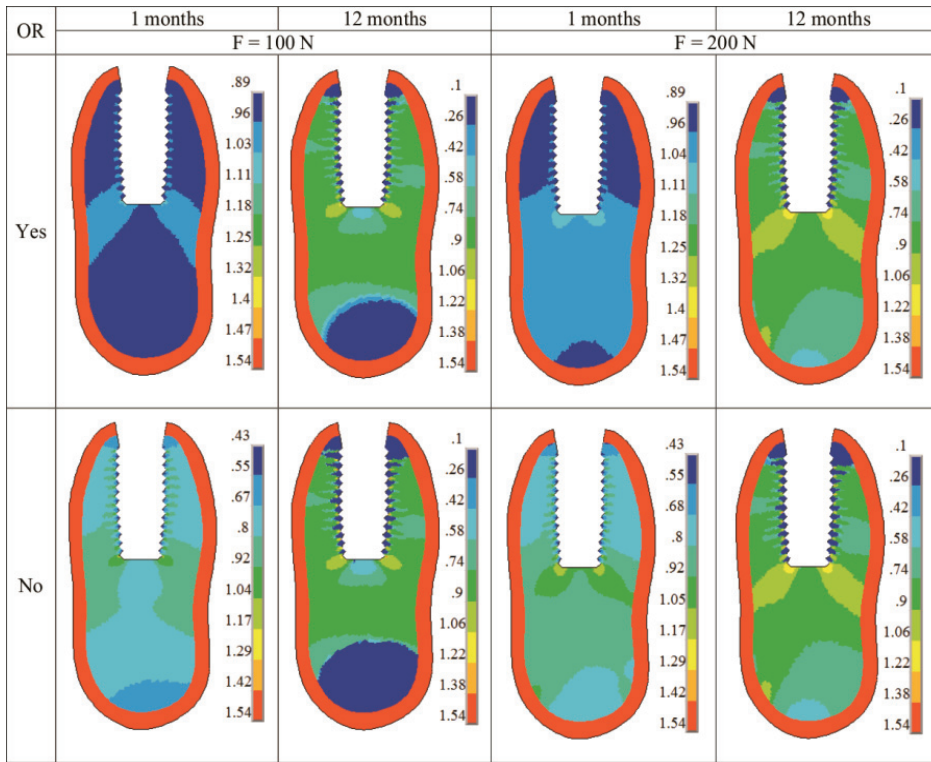


Fig. 4. Density distributions corresponding to Q1 BR simulations

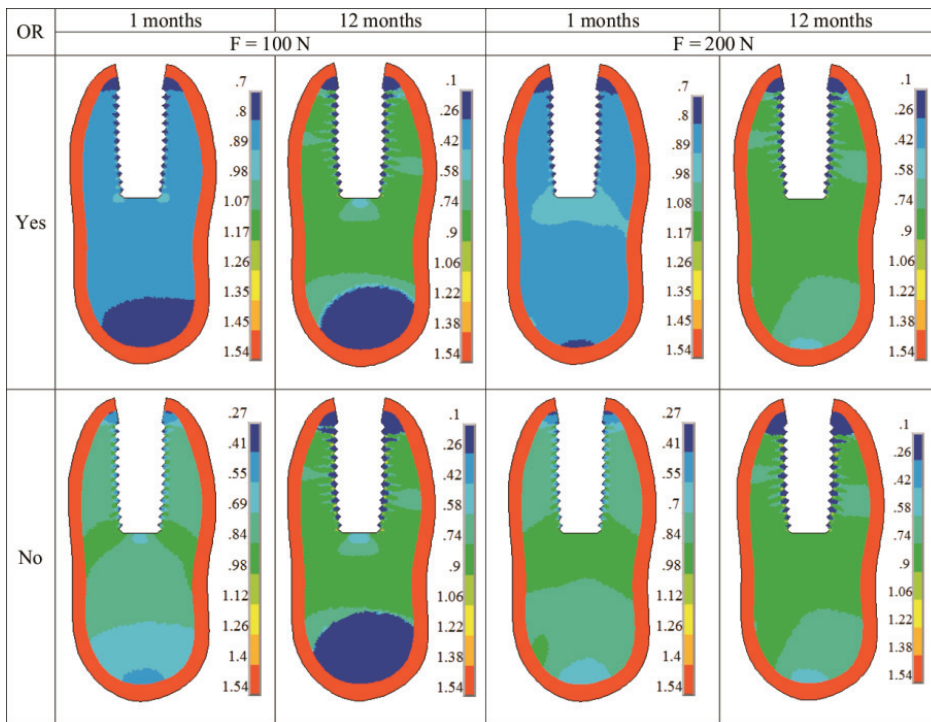


Fig. 5. Density distributions corresponding to Q2 BR simulations

Another interesting result was that different initial BQs generated close values of the final trabecular mass for the same loading force, although density distributions were different. This result is consistent with previous studies regarding the sensibility of the mathe-

tical model of BR to initial conditions [14], [17]. It can be concluded that there is an optimum bone quantity needed for a certain loading condition to be maintained within physiologically acceptable limits and different bone morphologies can ensure such quantity.



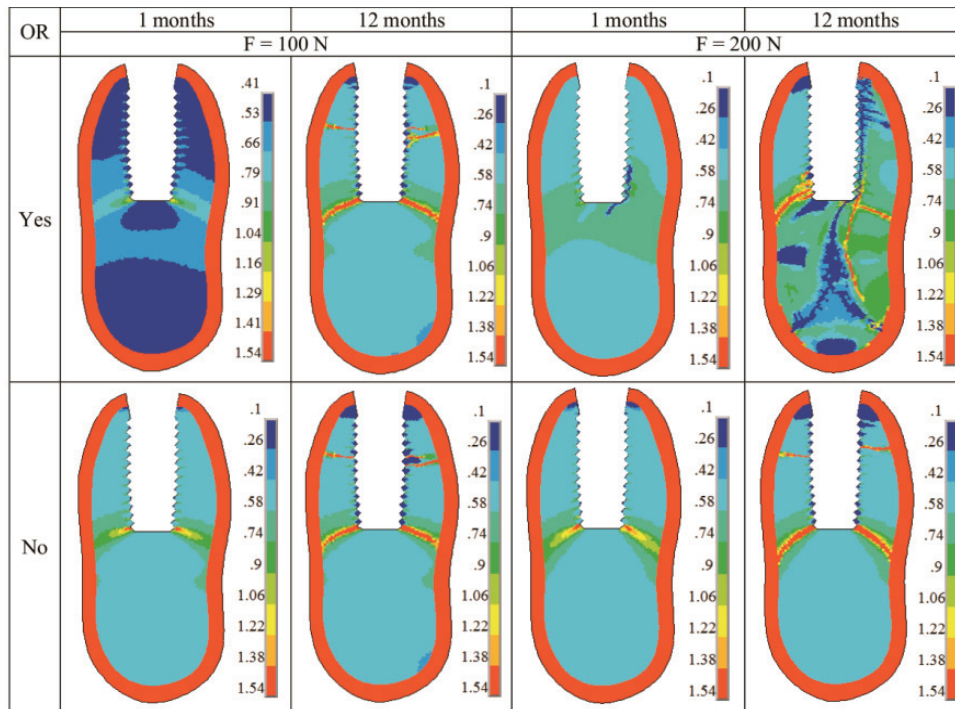


Fig. 6. Density distributions corresponding to Q3 BR simulations

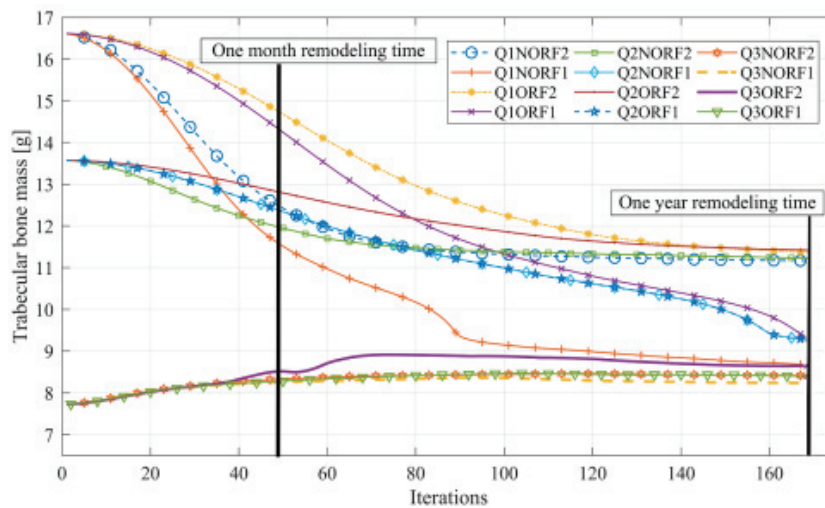


Fig. 7. Trabecular bone mass variation during simulation time

### 4. Discussion

Predictions of bone density redistribution due to mechanical interaction with the dental implants, based on computer simulations, became a field of interest in Computational Biomechanics, because it may give insights, among others, on how bone responds to different implant shapes, dimensions, materials, implanted position. Such knowledge would enable best implant selection, optimization or customization. In this context, the aim of this work is to correlate the

initial density distributions in BR models with data from clinics, according to which, prior to implantation, bone density is examined as an important factor for implant survival. Too low density does not ensure mechanical support for the implant, increasing the risk of implant failure.

In most simulations of BR around dental implants, initial bone density is homogenized over the analysis domain, resulting in a constant distribution. Usually, the constant is defined as half of the cortical density [2], [16], or follows values from other studies [9]–[11]. Because the simulations are intended to test mathe-

mathematical models and to check different correlations with the clinical data, such approach is convenient and sufficient. This work demonstrates that extending the goal of the simulations towards designing custom dental implants, optimization of existing ones or selecting from a given set, the initial density must be considered an important parameter in correlation with the OR.

Using a variable time step enables increasing the speed of the remodeling simulations, by reducing the number of iterations needed for convergence and keeping the truncation errors small. In previous studies, a constant time step small enough to assure mathematical precision was used, thus a high number of iterations were needed for convergence.

The limitations of the study are determined by the model dependence. The results are dependent on finite element model, initial Young's modulus values considered representative for the three BQs, occlusal loading, implant geometry, boundary conditions. For instance, increasing the loading force over 200 N may result in overload resorption also for medium quality of bone or for higher values in the low quantity interval. Also, by applying an inclined force, the occlusal load acts may increase the stresses, especially at the implant tip and, as a result, the Young's modulus initial values that generate overload resorption will be increased. Nevertheless, such an increase would not be too high due to the small value of the horizontal component of the occlusal force. Different quantitative model behavior is also expected by changing the BQ reference values of initial Young's modulus. However, by using average values for the representative initial Young's moduli, the results obtained indicate a correlation of numerical simulation with clinical reality. Thus, following quantitative imagistic data, the clinical bone density with the Young's modulus is equated, which determines the model initial stiffness and, therefore, the simulated remodeling process behavior.

The results presented here are also consistent with previous studies [18] which demonstrated that bone elastic modulus is an important parameter for selecting the proper implant due to the influence upon interface stress-strain states which determines bone remodeling process behavior.

## 5. Conclusions

This article demonstrates that the initial material properties are important parameters when simulating bone remodeling around dental implants, especially

when overload resorption prediction is employed. Theories that do not account for overload resorption may conduct to qualitative false results, because, regardless of the initial density, they predict highly growing density. Such results are not in accordance with the clinical reality, which often shows implant failure in low quality trabecular bone. Therefore, when applied to implant design or optimization, it is likely to obtain wrong designs.

## Acknowledgements

Part of the work has been funded by the Sectoral Operational Programme Human Resources Development 2007–2013 of the Ministry of European Funds through the Financial Agreement POSDRU/159/1.5/S/134398 by EEA Financial Mechanism 2009–2014 under the project EEA-JRP-RO-NO-2013-1-0123 – Navigation System for Confocal Laser Endomicroscopy to Improve Optical Biopsy of Peripheral Lesions in the Lungs (NAVICAD), contract no. 3SEE/30.06.2014.

## References

- [1] CARTER D.R., HAYES W.C., *The compressive behavior of bone as a two-phase porous structure*, J. Bone Joint Surg. Am., 1977, 59(7), 954–962.
- [2] CHOU H.Y., JAGODNIK J.J., MUFTU S., *Predictions of bone remodeling around dental implant systems*, J. Biomech., 2006, 41(6), 1365–1373.
- [3] FAEGH S., MÜFTÜ S., *Load transfer along the bone-dental implant interface*, J. Biomech., 2010, 43(9), DOI: 10.1016/j.jbiomech.2010.02.017.
- [4] FROST H.M., *Bone's Mechanostat: A 2003 Update*, Anat. Rec. A, 2003, 275(2), 1081–1101.
- [5] HASAN I., RAHIMI A., KEILIG L., BRINKMANN K.T., BOURAUUEL K., *Computational simulation of internal bone remodelling around dental implants: a sensitivity analysis*, Comput. Method Biomech., 2012, 15(8), 807–814.
- [6] HELGASON B., PERILLI E., SCHILEO E., TADDEI F., BRYNJÓLFSSON S., VICECONTI M., *Mathematical relationships between bone density and mechanical properties: A literature review*, Clin. Biomech., 2008, 23(2), 135–146.
- [7] HUISKENS R., WEINANS H., GROOTENBOER H., DALSTRA M., FUDALA B., SLOOFF T., *Adaptive bone remodeling theory applied to prosthetic design analysis*, J. Biomech., 1987, 20(11–12), 1135–1150.
- [8] LI J., LI H., SHI L., FOCK A.S., UCER C., DEVLIN H., HORNER K., SILIKAS N., *A mathematical model for simulating the bone remodeling process under mechanical stimulus*, Dent. Mater J., 2007, 23(9), 1073–1078.
- [9] LI W., LIN D., CHEN J., ZHANG Z., LIAO Z., SWAIN M., LI Q., *Role of Mechanical Stimuli in Oral Implantation*, J. Biosci. Med., 2014, 2(4), DOI: 10.1002/ar.1092190104.
- [10] LIAN Z., GUAN H., IVANOVSKI S., LOO Y.-C., JOHNSON N.W., ZHANG H., *Effect of bone to implant contact percentage on bone remodelling surrounding a dental implant*, Int. J. Oral Maxillofac. Surg., 2010, 39(7), DOI: 10.1016/j.ijom.2010.03.020.



- [11] LIN D., LI Q., LI W., DUCKMANTON N., SWAIN M., *Mandibular bone remodeling induced by dental implant*, J. Biomech., 2010, 43(2), 287–293.
- [12] MAVROGENIS A.F., DIMITROIU R., PARVIZI J., BABIS G.C., *Biology of implant osseointegration*, J. Musculoskelet Neuronal Interact., 2009, 9(2), 61–71.
- [13] MOLLY L., *Bone density and primary stability in implant therapy*, Clin. Oral Imp. Res., 2006, 17 (Suppl. 2), 124–135.
- [14] MULLENDER M.G., HUISKES R., *Proposal for the regulatory mechanism of Wolff's law*, J. Orthop. Res., 1995, 13(4), DOI: 10.1002/jor.1100130405.
- [15] NORTON M.R., GAMBLE C., *Bone classification: an objective scale of bone density using the computerized tomography scan*, Clin. Oral Implan. Res., 2001, 12(1), DOI: 10.1034/j.1600-0501.2001.012001079.
- [16] NUȚU E., GHEORGHIU H., *Influence of the numerical method on the predicted bone density distribution in element based simulations*, U.P.B. Sci. Bull. D., 2013, 75(2), 73–84.
- [17] NUȚU E., *Interpretation of parameters in strain energy density bone adaptation equation when applied to topology optimization of inert structures*, Mechanika, 2015, 21(6), DOI: 10.5755/j01.mech.21.6.12106.
- [18] ROY S., DAS M., CHAKRABORTY P., BISWAS J.K., CHATTERJEE S., KHUTIA N., SAHA S., CHOWDHURY A.R., *Optimal selection of dental implant for different bone conditions based on the mechanical response*, Acta Bioeng. Biomech., 2017, 19(2), 11–20.
- [19] RHO J.Y., HOBATHO M.C., ASHMAN R.B., *Relations of Mechanical Properties to Density and CT Numbers in Human Bone*, Med. Eng. Phys., 1995, 17(5), DOI: 10.1016/1350-4533(95)97314-F.
- [20] SANTOS M.C.L.G., CAMPOS M.I.G., LINE S.R.P., *Early dental implant failure: A review of the literature*, Braz. J. Oral Sci., 2002, 1(3), 103–111.
- [21] TANAKA E., YAMAMOTO S., NISHIDA T., AOKI Y., *A mathematical model of bone remodeling under overload and its application to evaluation of bone resorption around dental implants*, Acta Bioeng. Biomech., 1999, 1(1), 117–121.
- [22] VIDYASAGAR L., APSE P., *Biological response to dental implant loading/overloading. Implant overloading: Empiricism or science?*, Stomatologija, 2003, 5, 83–89.